https://doi.org/10.5194/hess-2020-224
Preprint. Discussion started: 22 July 2020

Hydrology and Earth System Sciences
Discussions
Open Access
EGU

Comparative analysis of Kernel-based versus BFGS-ANN and deep learning methods in monthly reference evaporation estimation

Mohammad Taghi SATTARI [1,2], Halit APAYDIN[3], Shahab SHAMSHIRBAND [4,5], Amir MOSAVI[6,7]

[1]Department of Water Engineering, Faculty of Agriculture, University of Tabriz, Tabriz 51666, Iran
[2]Institute of Research and Development, Duy Tan University, Danang 550000, Vietnam.
[3]Department of Agricultural Engineering, Faculty of Agriculture, Ankara University, Ankara 06110, Turkiye
[4]Department for Management of Science and Technology Development, Ton Duc Thang University, Ho Chi Minh City, Viet Nam
[5]Faculty of Information Technology, Ton Duc Thang University, Ho Chi Minh City, Viet Nam
[6]Faculty of Civil Engineering, Technische Universität Dresden, 01069 Dresden, Germany
[7]Department of Informatics, J. Selye University, 94501 Komarno, Slovakia

Correspondence to: Mohammad Taghi SATTARI (mtsattar@gmail.com, mtsattar@tabrizu.ac.ir)

Abstract. Proper estimation of the reference evapotranspiration (ET_0) amount is an indispensable matter for agricultural water management in the efficient use of water. The aim of study is to estimate the amount of ET_0 with a different machine and deep learning methods by using minimum meteorological parameters in the Corum region which is an arid and semi-arid climate with an important agricultural center of Turkey. In this context, meteorological variables of average, maximum and minimum temperature, sunshine duration, wind speed, average, maximum, and minimum relative humidity are used as input data monthly. Two different kernel-based (Gaussian Process Regression (GPR) and Support Vector Regression (SVR)) methods, BFGS-ANN and Long short-term memory models were used to estimate ET_0 amounts in 10 different combinations. According to the results obtained, all four methods used predicted ET_0 amounts in acceptable accuracy and error levels. BFGS-ANN model showed higher success than the others. In kernel-based GPR and SVR methods, Pearson VII function-based universal kernel was the most successful kernel function. Besides, the scenario that is related to temperature in all scenarios used, including average temperature, maximum and minimum temperature, and sunshine duration gave the best results. The second-best scenario was the one that covers only the sunshine duration. In this case, the ANN (BFGS-ANN) model, which is optimized with the BFGS method that uses only the sunshine duration, can be estimated with the 0.971 correlation coefficient of ET_0 without the need for other meteorological parameters.

https://doi.org/10.5194/hess-2020-224
Preprint. Discussion started: 22 July 2020


Hydrology and Earth System Sciences
Discussions

1 Introduction

It can be noted that water is one of the most important elements on earth that is used by every organism. Without water, it will become almost impossible to survive. It may easy to survive for a few days without getting enough meal but it is completely unable to survive without drinking water. For plants, water is the main requirement for its growth. It means that it is not easy to grow plants without giving them proper water. Furthermore, one of the most important facts is that water is helping the living organisms to maintain their body temperature. The next fact is that water also helps to absorb the nutrients efficiently. It is also used in dissolving nutrients. Another reason is that water is responsible for refraining from different kinds of diseases. With the help of water, it will become easy to maintain the body shape more effectively without any sort of problem.

Accurate estimation of reference crop evapotranspiration (ET_0) and crop water consumption (ET) is an important process for the management of water in agricultural sector in arid and semi-arid climatic conditions where water is scarce and valuable. Although ET_0 is a complex element of the hydrological cycle, it is also an important component of hydro-ecological applications and the water management in agricultural sector. ET_0 is important in increasing irrigation efficiency, irrigation planning and reuse of water. ET_0 estimation is an essential tool for the forcible management of irrigation and hydro-meteorological studies on the basin and national scale.

Many studies have been reported to introduce approaches for ET_0 estimation and to test these methods. ET_0 is considered a complex and nonlinear phenomenon that interacts with water, agriculture, and climate sciences. It is difficult to calculate such a phenomenon by experimental and classical mathematical methods. There are about twenty well-known methods for predicting ET_0 based on different meteorological variables and assumptions. Many of these methods commonly require input and output dataset. The Penman-Monteith (FAO56PM) method proposed by FAO is recommended to estimate ET_0, as it usually gives the best results in different climatic conditions (Feng et al. 2016, Nema et al 2017).

Today, it is seen that artificial intelligence techniques based on machine learning (ML) can successfully predict the processes showing a complex and nonlinear structure. It is witnessed that scientists frequently use artificial intelligence methods based on excess data in natural sciences, especially hydrology. Thus, methods such as ML, deep learning, and artificial intelligence have gained popularity in calculating and predicting ET_0, as can be seen from the literature search. Sattari et al. (2013) used the backpropagation algorithm of artificial neural network (ANN) and tree-based M5 model to estimate the monthly ET_0 amount by employing climate dataset in the Ankara region. As the input parameter, the monthly air temperature, total sunshine duration, relative humidity, precipitation, wind speed and monthly time index were used, while the ET_0 computed by FAO56PM was used as output for both approaches. The results revealed that the neural network approach gives better results with this data set. Citakoglu et al. (2014) predicted the monthly average ET_0 using the ANN and adaptive network-based fuzzy inference system (ANFIS) techniques. Different combinations of long-term average monthly climate data of wind speed, air temperature, relative humidity, and solar radiation recorded at the stations used as input data. According to the results of the study; Although ANFIS is slightly more successful than ANN, it has been found that both methods can be used in estimating the monthly mean ET_0. Wen et al. (2015) predicted the daily ET_0 amount by SVM method, using limited climate dataset in the

https://doi.org/10.5194/hess-2020-224
Preprint. Discussion started: 22 July 2020


Hydrology and Earth System Sciences
Discussions

region of China's extremely arid Ejina basin. In the study, the highest and lowest air temperatures, daily solar radiation and wind speed values were used as model input and FAO56PM results as model output. Besides, the performance of the SVM method was compared to ANN and empirical techniques, including Hargreaves, Priestley-Taylor and Ritchie. The results indicated that among these models, the SVM provided the highest performance. Gocic et al. (2015) determined ET_0 using the FAO56PM method using data from 1980-2010. They used four different computational intelligence methods: Genetic programming (GP), SVM-Firefly algorithm (SVM-FFA), ANN, and SVM-Wavelet. While this study shows that the hybrid SVM-Wavelet provides the highest accuracy for the estimation of ET_0; It is determined that SVM-Wavelet followed by the hybrid SVM-FFA provide the higher correlation coefficient compared to ANN and GP. Feng et al. (2016) used trained extreme-learning machine (ELM), the integration of genetic algorithm-ANN (GA-ANN) and wavelet neural networks (WNN) to predict ET_0 in a humid basin of Southeast China. The results were compared with empirical ET_0 (temperature-based i.e. Hargreaves and modified Hargreaves and radiation-based i.e. Makkink, Priestley-Taylor, and Ritchie). Results found that ELM and GANN are better than WNN models. It has been determined that temperature-based ELM and GANN have higher accuracy than Hargreaves and modified Hargreaves, and radiation-based ELM and GANN have higher performance than Makkink. Shamshirband et al. (2016) estimated ET_0 with ANN and ANFIS models by employing the Cuckoo search algorithm (CSA). In the study, the models of monthly climate data from the twelve meteorological stations in Serbia were used as input in the 1983-2010 period. For the study, they chose the FAO56PM equation as the ET_0 equation. The results showed that the hybrid ANFIS-CSA can be employed for high-reliability ET_0 estimation. Pandey et al. (2017) in their study, ML techniques for ET_0 estimation using limited meteorological data; evaluated evolutionary regression (ER), ANN, multiple nonlinear regression (MLNR), and SVM. According to the results of the study, the ANN FAO56PM model performed better. In their study, Nema et al. (2017) studied the possibilities of using ANN to increase the performance of monthly evaporation prediction in the humid area of Dehradun. They developed different ANN models including combinations of various educational functions and neuron numbers and compared them with ET_0 calculated with FAO56PM. According to the results, the ANN trained by Levenberg-Marquardt algorithm with nine neurons in a single hidden layer made the best estimation performance. Feng et al. (2017) estimated the daily ET_0 using temperature data, by employing ELM and generalized regression neural network (GRNN) at six meteorological stations in the southwestern Sichuan basin in China. In the study, ET_0 determined by FAO56PM and Hargreaves (HG) model for comparison. Two different scenarios were evaluated for ET_0 estimation. ELM and GRNN models gave acceptable results. Fan et al. (2018) used four models based on SVM, ELM, and decision tree to predict daily reference evaporation, using a limited number of meteorological data in various climates of China. Considering the complexity level and estimation performance, Extreme Gradient Boosting (XGBoost) and Gradient Boosting Decision Tree (GBDT) models found to be suitable methods for the prediction of daily ET_0. Banda et al. (2018) estimated the daily ET_0 for the Bulawayo Goetz region from climate data using neurocomputing methods and compared them with experimental methods. According to the results of the study, neurocomputing calculation techniques were found to be superior to empirical methods. Wu et al. (2019) estimated ET_0 using ANN, Random Forest (RF), GBDT, XGBoost, Multivariable Adaptive Regression Spline (MARS), Support Vector Regression (SVR) in the presence of temperature data. The results of the employed models were compared

https://doi.org/10.5194/hess-2020-224
Preprint. Discussion started: 22 July 2020


Hydrology and Earth System Sciences
Discussions

with those of the temperature-based Hargreaves-Samani equation. The research found that the success of ML techniques differs depending on the scenarios. Tree-based models (RF, GBDT, and XGBoost) provided higher prediction performance than rest of the models. Reis et al. (2019) also used Hargreaves Samani, ANN, multiple linear regression (MLR), and ELM models to predict ET_0 in the presence of temperature data in the Verde Grande River basin in southeastern Brazil. The results revealed that artificial intelligence methods have superiority over other models. Wang (2019) estimated the amount of ET_0 using PSO and least squares (LSSVM) models, based on the Hilbert-Huang transformation, using daily data from 2000-2009 of China's Hetian Xinjiang meteorological station. Under the condition of the working area, the accuracy of the ML techniques was found to be higher than those of the empirical models. Abrishami et al. (2019) estimated the amount of daily ET for wheat and corn by the ANN method. Leaf area index, daily climate data and plant height were employed as the input parameters. The results indicated the proper capacity and acceptable performance of ANNs with two hidden layers. Zhang et al. (2019) examined SVM's success in ET_0 estimation. The results were compared with Hargreaves, FAO-24, Priestley-Taylor, McCloud, and Makkink. SVM was determined to be the most successful model. Saggi et al. (2019) used deep learning and ML techniques in Punjab's Hoshiarpur and Patiala regions to determine daily ET_0. In the study, supervised learning algorithms including Deep Learning-Multilayer Sensors (DL), Random Forest (RF), Generalized Linear Model (GLM) and Gradient-Boosting Machine (GBM) were tested. In the study, it was determined that the DL model offers high performance for daily ET_0 modeling. Shabani et al. (2020) used ML methods including Gauss Process Regression (GPR), RF, and SVR, in the presence of meteorological data related to Iran to estimate evaporation (PE) and compare it with the measured values. The results showed that PE can be estimated using ML methods with a high performance and a small number of meteorological parameters that can be easily measured.

Corum region, with a total annual rainfall of 427 mm, can be classified as an arid and semi-arid region of Turkey. Proper prediction of reference evaporation is important to manage limited water resources for optimum agricultural production. ET_0 is one of the most important elements in water, agriculture, hydrology, and meteorology studies, and its determination is a very important process. ET_0 modeling is called as a complex and nonlinear phenomenon according to the interactions of climate factors. For this reason, ML, deep learning, and artificial intelligence methods have gained importance and popularity in this field.

This study has three important goals. In Corum conditions, which are arid and semi-arid climate, the amount of ET_0 was estimated by four machine and deep learning (GPR, SVR, hybrid ANN optimized with the Broyden – Fletcher – Goldfarb – Shanno approach (BFGS-ANN) and Long Short-Term Memory (LSTM)) method and the methods used were compared for the first time. Secondly, the effect of different kernel functions on SVR and GPR models results was investigated in ET_0 estimation. Finally, determining the model that provides the highest performance with the least meteorological variable requirement for the study.

https://doi.org/10.5194/hess-2020-224
Preprint. Discussion started: 22 July 2020

Hydrology and Earth System Sciences
Discussions

2 Material and method

2.1 Study area and dataset used

The surface area of Corum is 1 278 381 ha, of which 553 011 ha, or 43%, is agricultural land. Its population is 525 180 and 27% of it lives in rural areas. The water resource potential of the city is 4 916 hm^3/year and 84 988 ha of agricultural land is being irrigated. The main agricultural products are wheat, paddy, chickpeas, onions, walnuts, and green lentils. This study was conducted using the meteorological values measured from January 1993 - December 2018 in Corum province (Anonymous, 2017). Data used monthly are average, highest and lowest temperature, sunshine duration, wind speed, average, highest, and lowest relative humidity. 200 of the total 312 months of data were used for training and the remaining 112 were used for testing. Statistics of the data used are given in Table 1. The frequencies of meteorological data of the study area are given in Figure 1. As it is understood from the figure, the dependent variable ET_0 values do not conform to the normal distribution.

Table 1 Basic statistics of the data used in the study

Statistic	Tmean (^{0}c)	Tmax (^{0}c)	Tmin (^{0}c)	n (hr)	U (m/s)	RHmean (%)	RHmin (%)	RHmax (%)	ET_0 (mm/month)
Minimum	-6.18	-1.27	-11.30	0.83	0.70	66.87	19.03	45.80	11.76
Maximum	25.06	35.44	15.63	11.97	2.69	99.83	82.83	94.74	185.59
Mean	11.03	18.39	4.34	6.09	1.69	88.6	44.99	69.58	79.17
Stdev	7.96	9.29	6.33	2.96	0.41	5.81	13.2	9.38	52.86
Number of records	312	312	312	312	312	312	312	312	312

https://doi.org/10.5194/hess-2020-224
Preprint. Discussion started: 22 July 2020

Hydrology and Earth System Sciences
Discussions

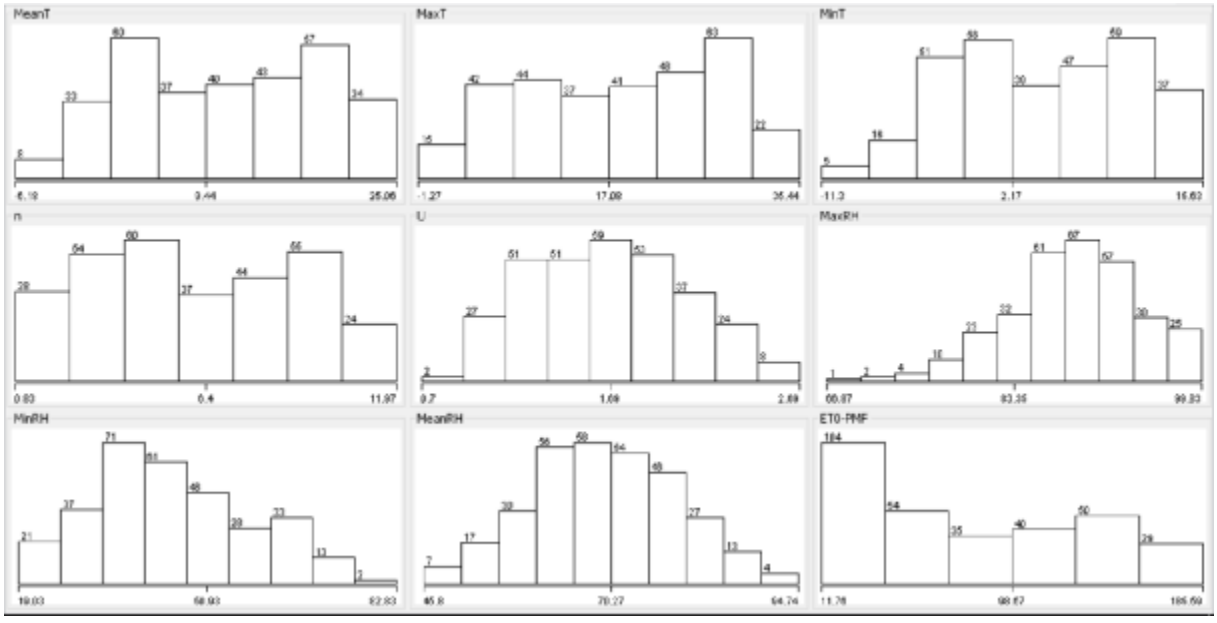

Figure 1. Frequencies of the variables used

To determine the meteorological factors employed in the model and the formation of scenarios, the relationship between ET_0 and other variables is given in Figure 2. As can be understood visually, the meteorological variables associated with temperature and especially the sunshine duration have a high correlation with ET_0. Considering these relationships, 10 different input scenarios were created and the effect of meteorological variables on ET_0 estimation was evaluated. Table 2 gives the meteorological variables used in each scenario.

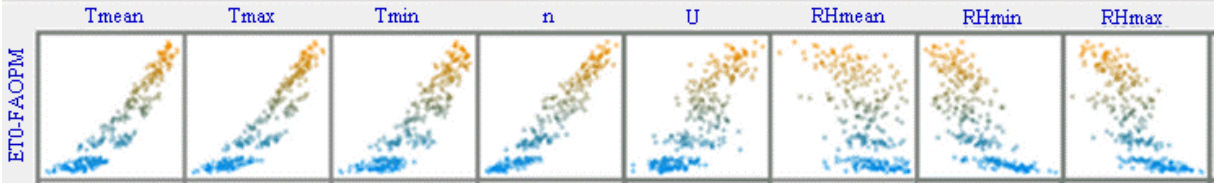

Figure 2. Correlation between ET_0 and independent variables

https://doi.org/10.5194/hess-2020-224
Preprint. Discussion started: 22 July 2020


Hydrology and Earth System Sciences
Discussions

Table 2. Variables used in scenarios

Scenario	Inputs
1	TMean, TMax, TMin ,n, U, RHMax, RHMin, RHMean
2	TMean, n, U, RHMean
3	TMax, n, RHMax
4	TMax,n , U
5	TMean, TMax, TMin, n
6	n, U, RHMax
7	n, RHMax
8	n
9	TMin
10	TMax

3 Methods

3.1 Calculation of ET_0

The United Nations, Food and Agriculture Organization (FAO) have recommended Penman-Monteith (PM) equation (Eq.1) to calculate evapotranspiration of reference crop (Doorenbos and Pruitt, 1977). Although the PM equation is much more complex than the other equations, it has been formally explained by FAO. The equation has two main features: (1) It can be used in any weather conditions without local calibration, and (2) the performance of the equation is based on the lysimetric data in an approved spherical range. Requirement for the many of meteorological factors can be defined as the main problem. However, in many countries, there is still no equipment to record these parameters correctly, or data is not regularly recorded (Gavili et al., 2018).

$$ET_0 = \frac{0.408\,\Delta\,(R_n - G) + \gamma \frac{900}{T+273} u_2 (e_s - e_a)}{\Delta + \gamma(1 + 0.34 u_2)} \qquad \text{(Eq.1)}$$

Where

ET_0 refers to the reference evapotranspiration [mm day^{-1}],

G refers the soil heat flux density [MJ m^{-2} day^{-1}],

u_2 refers to the wind speed at 2 m [m s^{-1}],

e_a referes to the actual vapour pressure [kPa],

e_s refers to the saturation vapour pressure [kPa],

https://doi.org/10.5194/hess-2020-224
Preprint. Discussion started: 22 July 2020


Hydrology and Earth System Sciences
Discussions

e_s-e_a refers to the saturation vapour pressure deficit [kPa],

T refers to the mean daily air temperature at 2 m [∘C],

Rn refers to the net radiation at the crop surface [MJ m^{-2} day^{-1}],

γ refers to the psychrometric constant [kPa ∘C^{-1}],

Δ refers to the slope vapour pressure curve [kPa ∘C^{-1}].

3.2 BFGS-ANN

In this study, the hybrid neural network method (BFGS-ANN) optimized with the Broyden – Fletcher – Goldfarb – Shanno approach was used to estimate ET_0 amounts. In optimization studies, the Broyden–Fletcher–Goldfarb–Shanno (BFGS) method is a repetitious approach for solving unlimited nonlinear optimization problems (Fletcher, 1987). The hybrid BFGS-ANN technique trains a multilayer perceptron ANN with one hidden layer by reducing the given cost function plus a quadratic penalty with the (BFGS) technique. The BFGS approach includes Quasi-Newton methods. For such problems, the required condition for reaching an optimal level accures when the gradient is zero. Newton and the BFGS methods cannot be guaranteed to converge unless the function has a quadratic Taylor expansion near an optimum. However, BFGS can have a high accuracy even for non-smooth optimization instances (Curtis et al. 2015).

Quasi-Newton methods do not compute the Hessian matrix of second derivatives. Instead, the Hessian matrix is drawn by updates specified by gradient evaluations. Quasi-Newton methods are extensions of the secant method to reach the basis of the first derivative for multi-dimensional problems. In multi-dimensional problems, the secant equation does not specify a certain solution, and Quasi-Newton methods differ in how to limit the solution. The BFGS method is one of the frequently used members of this class (Nocedal and Wright 2006). In the BFGS-ANN method application all attributes including the target attribute (meteorological variables and ET_0) are standardized. In the output layer, the sigmoid function employed for classification. In approximation, the sigmoidal function can be specified for both hidden and output layers. For regression, the activation function can be employed as the identity function in the output layer.

3.3 SVR

The statistical learning theory is the basis of the SVM. The optimum hyperplane theory and kernel functions and nonlinear classifiers were added as linear classifiers (Vapnik 2013). Models of the SVM are separated into two main categories: (a) The classifier SVM and (b) the SVR model. An SVM is employed for the classification of data in various classes, and the SVR is employed for estimation problems. Regression is used to take a hyperplane suitable for the data used. The distance to any point in this hyperplane shows the error of that point. The best technique proposed for linear regression is the least-squares (LS) method. However, it may be completely impossible to use LS estimator in the presence of outliers. In this case, a robust predictor have to be developed that will not be sensitive to minor changes, as the processor will perform poorly.

https://doi.org/10.5194/hess-2020-224
Preprint. Discussion started: 22 July 2020


Hydrology and Earth System Sciences
Discussions

3.4 GPR

The Gauss process (GP) is defined by Rasmussen and Williams (2005) as follows: A GP is a complex of random variables, any limited number of which have a joint Gaussian distribution. Kernel-based methods such as SVM and GPs can work together to solve flexible and applicable problems. The GP explained by two functions: Average and covariance functions (Eq. 2). The average function is a vector; the covariance function is a matrix. The GP model is a possibly nonparametric black box technique.

$$f \approx GP(m, k) \quad \text{(Eq. 2)}$$

Where f refers to Gauss distribution, m refers to a mean function and k refers to covariance function.
The value of covariance expresses the correlation between the individual outputs concerning the inputs. The covariance value determines the correlation between individual outputs and inputs. The covariance function produces a matrix of two parts (Eq.3).

$$Cov(x_p) = C_f(x_p) + C_n(x_p) \quad \text{(Eq. 3)}$$

Here C_f represents the functional part, but defines the unknown part of the modeling system, while C_n represents the noise part of the system. A Gaussian process (GP) is closely related to SVM and both are part of the kernel machine area in ML models. Kernel methods are sample-based learners. Instead of learning a fixed parameter, the kernels memorize the training data sample and assign a certain weight to it.

3.5 Long short-term memory (LSTM)

LSTM is a high-quality evolution of Recurrent Neural Networks (RNN). This neural network is presented for addressing the problems that were present in RNN and this had been done through adding more interactions per cell. These systems are also a special one because it contains remembering information from a long period. Moreover, it also contains four basic interacting layers and all of them contain the different methods of communication. Its main structure can be explained with the help of Figure 3 (Le et al., 2019, Brownlee, 2020).

https://doi.org/10.5194/hess-2020-224
Preprint. Discussion started: 22 July 2020

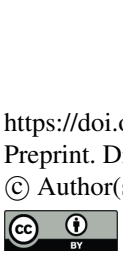

Hydrology and Earth System Sciences
Discussions

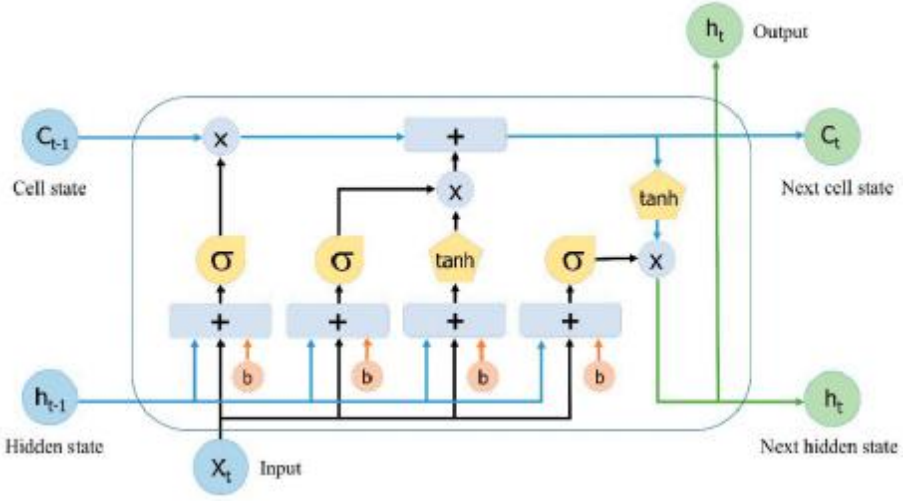

240 Figure 3. LSTM Architecture (Brownlee, 2020)

The next thing is that its complete network consists of a memory block. These blocks are also called as cells. The information is stored in one cell and then transferred into the next one with the help of gate controls. Through the help of these gates, it will become extremely easy to analyze the information accurately. All of these gates are extremely important and they are
245 called forget gates. This can be explained with the help of Eq. 4.

$$f_t = \sigma\left(W_f[h_{t-1}, X_t] + b_f\right) \quad \text{(Eq. 4)}$$

LSTM units or blocks are part of the repetitive neural network structure. Repetitive neural networks are made to use some
250 artificial memory processes that can help these AI programs mimic human thinking more effectively.

3.6 Kernel functions

In this study, as given in Table 3, four different kernel functions that are frequently included in the literature were used. The polynomial, radial-based function, Pearson VII function (PUK), and normalized polynomial kernels used and their formulas and parameters are tabulated in Table 3. As is clear from Table 3, some parameters must be determined by the user for each
255 kernel function. While the number of parameters to be determined for PUK kernel is two, it requires the determination of a parameter in the model formation that will be the basis for classification for other functions. When kernel functions are compared, it is seen that polynomial and radial based kernels are more plain and understandable. Although it may seem mathematically simple, the increase in the degree of the polynomial makes the algorithm complex. This significantly increases processing time and decreases the classification accuracy after a point. In contrast, changes in the parameter (γ) of the radial-
260 based function, expressed as the kernel size, were less effective on classification performance (Hsu et al., 2010). The

https://doi.org/10.5194/hess-2020-224
Preprint. Discussion started: 22 July 2020


Hydrology and Earth System Sciences
Discussions

normalized polynomial function was proposed by Arnulf et al. (2001) in order to normalize the mathematical expression of the polynomial kernel instead of normalizing the data set.

It can be said that the normalized polynomial kernel is a generalized version of the polynomial kernel. On the other hand, PUK kernel has a more complex mathematical structure than other kernel functions with its two parameters (σ, ω) known as Pearson width. These two parameters affect classification accuracy and it is not known in advance which parameter pair will perform best. For this reason, determining the most suitable parameter pair in the use of PUK kernel is an important step.

Table 3. Basic kernel functions and parameters used in SVM

Kernel functions	Mathematical Expression	Parameter
Polynomial kernel	$K(x,y) = \left((x.y) + 1\right)^d$	Polynomial degree (d)
Normalized polynomial kernel	$K(x,y) = \frac{\left((x.y) + 1\right)^d}{\sqrt{\left((x.x) + 1\right)^d \left((y.y) + 1\right)^d}}$	Polynomial degree (d)
Radial Based Function Kernel	$K(x,y) = e^{-\gamma\lvert(x-x_i)\rvert^2}$	Kernel size (γ)
PUK	$K(x,y) = \frac{1}{\left[1 + \left(\frac{2.\sqrt{\lVert x-y\rVert^2}\ \sqrt{2^{(1/\omega)}-1}}{\sigma}\right)^2\right]^{\omega}}$	Pearson width parameters (σ, ω)

The editing parameter C must be determined by the user for all SVM during runtime. If values that are too small or too large for this parameter are selected, the optimum hyperplane cannot be determined correctly, therefore there will be a serious decrease in classification accuracy. On the other hand, if C equal to infinity, the SVM model becomes suitable only for datasets that can be separated linearly. As can be seen from here, the selection of appropriate values for the parameters is a variable that directly affects the accuracy of the SVM classifier. Although a trial and error strategy is generally used, the cross-validation approach enables successful results. The purpose of the cross-validation approach is to determine the performance of the classification model created. For this purpose, the data is separated into two categories. While the first part is used as training data in a model form that is the basis for classification, the second part is processed as test data to determine the performance of the model. As a result of applying the model created with the training set to the test data set, the number of samples classified correctly indicates the performance of the classifier. Therefore, by using the cross-validation method, the model that will be the basis for classification and determination of the kernel parameters, in which the best classification performance is obtained, was created (Kavzoglu ve Golkesen, 2010).

https://doi.org/10.5194/hess-2020-224
Preprint. Discussion started: 22 July 2020


Hydrology and Earth System Sciences
Discussions

3.7 Model Evaluation

Some common statistical parameters were used in the selection and comparison of the models used in the study. Differences between ET_0 data determined by the root mean square error (RMSE), mean absolute error (MAE) and correlation fit (R) via Eq. 5-7. Here, X_i and Y_i are the observed and predicted values, and N is the number of data.

$$MAE = \frac{1}{N}\sum_{i=1}^{N}|X_i - Y_i| \quad \text{(Eq. 5.)}$$

$$RMSE = \sqrt{\frac{1}{N}\Sigma_{i=1}^{N}(X_i - Y_i)^2} \quad \text{(Eq. 6.)}$$

$$R = \frac{N\sum X_i Y_i - (\sum X_i)(\sum Y_i)}{\sqrt{N(\sum X_i^2) - (\sum X_i)^2}\sqrt{N(\sum Y_i^2) - (\sum Y_i)^2}} \quad \text{(Eq. 7.)}$$

Also, Taylor diagrams applied to check the performance of the used models. In this diagram, observed and statistical parameters can be detected simultaneously. Moreover, various points on the polar graph used to study the adaption between measured and predicted values in the Taylor diagrams. Besides, CC and normalized standard deviation are indicated by the azimuth angle and radial distances from the base point, respectively (Taylor 2001).

4. Results

In this study, 10 different alternative scenarios were created by using monthly average, highest and lowest temperature, sunshine time, wind speed, average, highest, and lowest relative humidity data. ET_0 amounts were estimated with the help of kernel-based GPR and SVR methods, BFGS-ANN, and one of the deep learning methods LSTM models. ET_0 estimation results obtained from different scenarios according to the GPR method are summarized in Table 4.

As can be seen from the chart, the 5th scenario including TMax, TMin, TMean and n containing four meteorological variables with the GPR method PUK function (R = 0.982, MAE = 9.947 mm/month, RMSE = 11.2109 mm/month) gave the best result. However, the 8th scenario with only one meteorological variable (sunshine duration) and an appropriate result (R = 0.9691, MAE = 11.8473 mm/month, RMSE = 15.8719 mm/month). Since the scenario with the least input parameters and with an acceptable level of accuracy can be preferred, scenario 8 was chosen as the optimum scenario.

The scatter plot and time series plots of the test phase for scenario 5 and 8 are given in Figures 4 and 5. As can be seen from the figure, a relative agreement has been achieved between the FAO56PM ET_0 values and the ET_0 values modeled. When the time series graphs are examined, minimum points in estimated ET_0 values are more in harmony with FAO56PM values than maximum points.

https://doi.org/10.5194/hess-2020-224
Preprint. Discussion started: 22 July 2020

Hydrology and Earth System Sciences
Discussions
Open Access
EGU

Table 4. Results obtained with GPR method

Scenario No	Kernel function	R	MAE (mm/month)	RMSE (mm/month)
1	Polynomial	0.9193	17.8013	21.4952
	PUK	0.9750	10.5906	13.4330
	Radial basis function	0.9602	22.3353	25.4332
2	Polynomial	0.9128	19.4655	23.9183
	PUK	0.9818	8.9058	11.5185
	Radial basis function	0.9678	27.5940	31.2150
3	Polynomial	0.8836	21.2623	26.2083
	PUK	0.9662	12.2152	15.0187
	Radial basis function	0.9525	31.9344	36.1935
4	Polynomial	0.8429	36.6604	41.2745
	PUK	0.9813	9.3003	12.4647
	Radial basis function	0.9742	29.7864	33.6709
5	Polynomial	0.7765	33.8278	38.3742
	PUK	0.9820	9.1947	11.2109
	Radial basis function	0.9612	26.2766	30.0768
6	Polynomial	0.8855	21.5210	27.2959
	PUK	0.9696	12.1685	15.8165
	Radial basis function	0.9482	33.4845	37.9140
7	Polynomial	0.8861	21.7258	26.9480
	PUK	0.9649	12.9590	16.5650
	Radial basis function	0.9352	36.9353	41.6716
8	Polynomial	0.9634	40.4306	45.9593
	PUK	0.9691	11.8473	15.8719
	Radial basis function	0.9634	37.6298	42.3803
9	Polynomial	0.9154	43.9357	50.0790
	PUK	0.9292	16.2747	20.1854
	Radial basis function	0.9154	40.0566	44.8850
10	Polynomial	0.9352	42.6604	48.7584
	PUK	0.9555	13.0145	15.8309
	Radial basis function	0.9353	39.1677	43.9253

https://doi.org/10.5194/hess-2020-224
Preprint. Discussion started: 22 July 2020

Hydrology and Earth System Sciences
Discussions

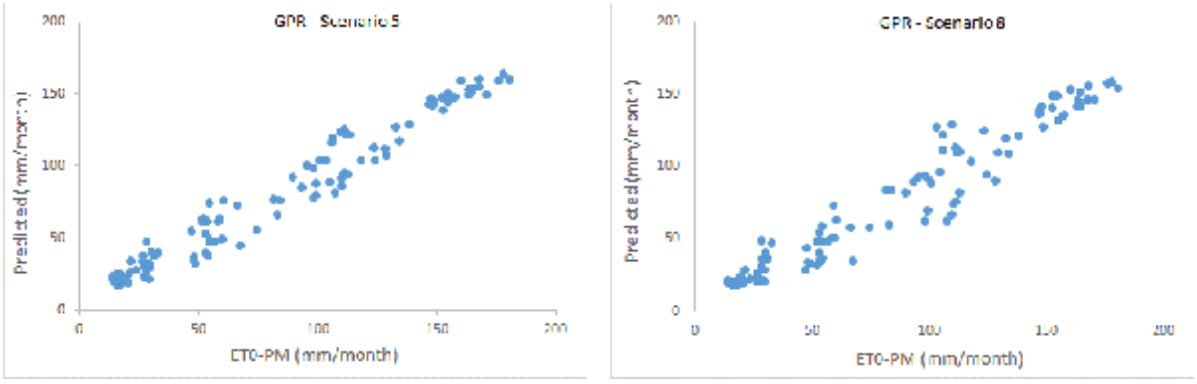

Figure 4. Scatter plots of scenarios 5 and 8

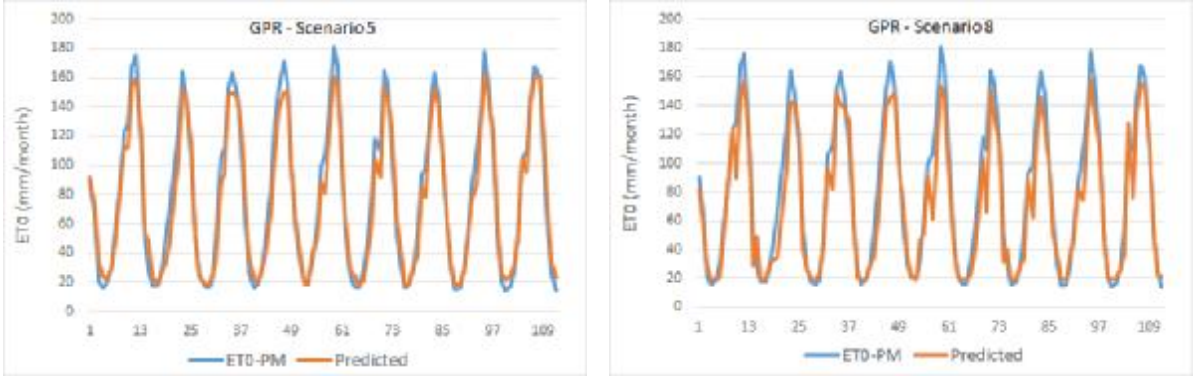

Figure 5. Time series graphics of Scenarios 5 and 8

Within the SVR model, 3 different kernel functions were evaluated in scenarios under the same conditions, and the results obtained are given in Table 5.

As can be seen here, scenarios 5 and 8 have yielded the best and most appropriate results according to the PUK function. According to the results, the 5th scenario including TMean, TMin, TMax and n meteorological variables gave the best result (R = 0.9885, MAE = 7.07 mm/month, RMSE = 9.3259 mm/month). However, scenario 8 gave the most appropriate result (R = 0.9691, MAE = 11.2408 mm/month, RMSE = 15.5611 mm/month) only with the meteorological variable of sunshine duration (n). Although the accuracy rate of the 8th scenario is somewhat lower than the 5th scenario, it provides convenience and is preferred in terms of application and calculation since it requires a single parameter. The sunshine duration can be measured easily and without the need for excessive costs and personnel, so that with just one parameter, the amount of ET_0 is estimated within acceptable accuracy limits.

https://doi.org/10.5194/hess-2020-224
Preprint. Discussion started: 22 July 2020


Hydrology and Earth System Sciences
Discussions

Table 5. Results obtained with the SVR method

Scenario No	Kernel function	R	MAE	RMSE
1	Polynomial	0.9826	11.0033	13.5740
	PUK	0.9840	8.70480	11.1693
	Radial basis function	0.9678	11.1203	13.4468
2	Polynomial	0.9760	10.1138	11.6124
	PUK	0.9870	8.88250	11.6469
	Radial basis function	0.9724	11.4313	13.5386
3	Polynomial	0.9571	13.5919	15.903
	PUK	0.9617	12.0206	15.6733
	Radial basis function	0.9543	15.1051	18.4364
4	Polynomial	0.9739	11.8516	14.1386
	PUK	0.9800	9.2452	12.5707
	Radial basis function	0.9747	12.6226	16.1700
5	Polynomial	0.9827	8.5349	10.2108
	PUK	0.9885	7.0700	9.3259
	Radial basis function	0.9653	11.8607	14.4412
6	Polynomial	0.9634	14.5901	17.9626
	PUK	0.9745	11.2859	14.7455
	Radial basis function	0.9550	16.7198	22.2031
7	Polynomial	0.9599	14.7185	17.6297
	PUK	0.9699	12.0180	15.5924
	Radial basis function	0.9461	19.4352	25.7907
8	Polynomial	0.9634	13.7164	16.4672
	PUK	0.9691	11.2408	15.5611
	Radial basis function	0.9634	19.1426	25.6111
9	Polynomial	0.9154	17.9619	22.8538
	PUK	0.9286	16.2552	20.9296
	Radial basis function	0.9154	26.4915	31.2574
10	Polynomial	0.9352	15.2039	19.8289
	PUK	0.9531	12.0109	16.8281
	Radial basis function	0.9353	23.7460	28.7051

325

The scatter plot and time series graph drawn for the SVR model is given in Figure 6 and 7. As can be seen from the figure, except for the less frequent endpoints, the other points are compatible with FAO56PM - ET_0 values and ET_0 values estimated from the model.

https://doi.org/10.5194/hess-2020-224
Preprint. Discussion started: 22 July 2020

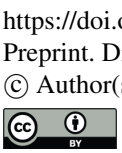

Hydrology and Earth System Sciences
Discussions

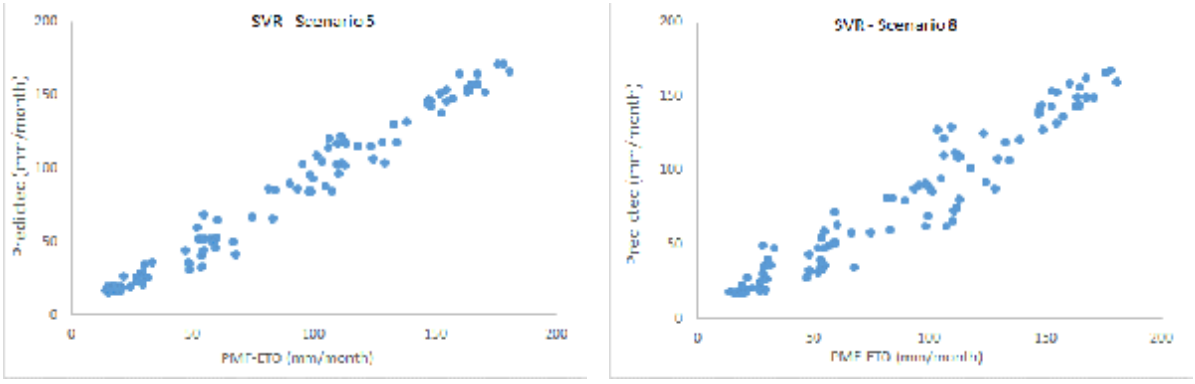

Figure 6. Scatter plots of scenarios 5 and 8

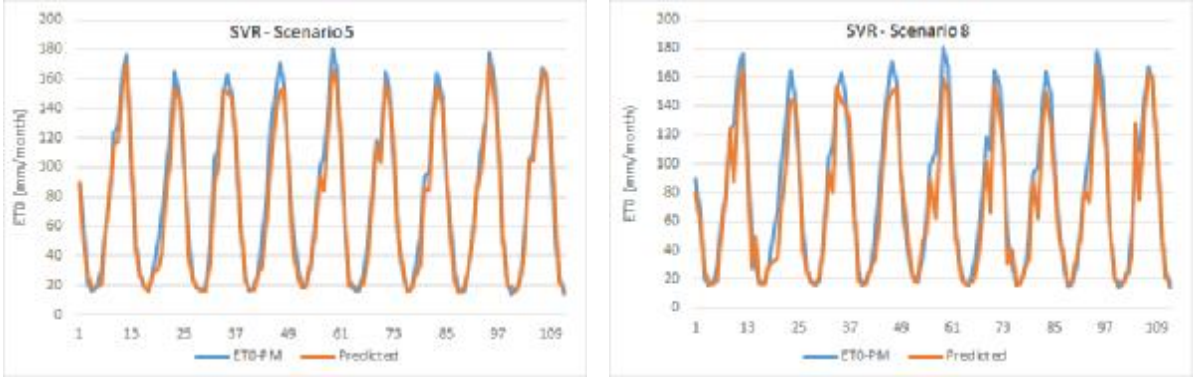

Figure 7. Time series graphics of Scenarios 5 and 8

330

In this study, ANN was optimized with the BFGS method and ET_0 amounts were estimated for all scenarios and the results are given in Table 6. In the implementation of the BFGS-ANN method, all features, including target feature (meteorological variables and ET_0), are standardized. In the hidden and output layer, the sigmoid function is f (x) = 1 / (1 + e ^ (- x)) used for classification.

335 As can be seen here, scenarios 5 and 8 have given the best and most appropriate results. According to the results, the 5th scenario including TMean, TMin, TMax and n meteorological variables gave the best result (R = 0.989, MAE = 6.7885 mm/month RMSE = 8.8991 mm/month). However, Scenario 8 gave the most appropriate result (R = 0.971, MAE = 11.4761 mm/month, RMSE = 15.6399 mm/month) with only the sunshine duration (n) meteorological variable. Although the accuracy rate of the 8th scenario is less than the 5th scenario, it is easy and practical in terms of application and calculation since it

340 consists of only one parameter. The scatter plot and time series graph drawn for the BFGS-ANN model is given in Figures 8 and 9. As can be seen, the BFGS-ANN method predicted ET_0 amounts with a high success rate, and a high level of agreement was achieved between the estimates obtained from the model and FAO56PM- ET_0 values.

https://doi.org/10.5194/hess-2020-224
Preprint. Discussion started: 22 July 2020

Table 6. Results obtained with BFGS-ANN method

Scenario No	Evaluation metrics		
	R	MAE	RMSE
1	0.9884	6.6346	8.6243
2	0.9849	7.5305	10.3722
3	0.9707	11.2870	14.3732
4	0.9828	9.1159	12.4740
5	0.9890	6.7885	8.8991
6	0.9758	11.5089	14.7687
7	0.9704	11.9444	15.7787
8	0.9710	11.4761	15.6399
9	0.9332	15.9139	19.8957
10	0.9565	12.4874	15.5428

345

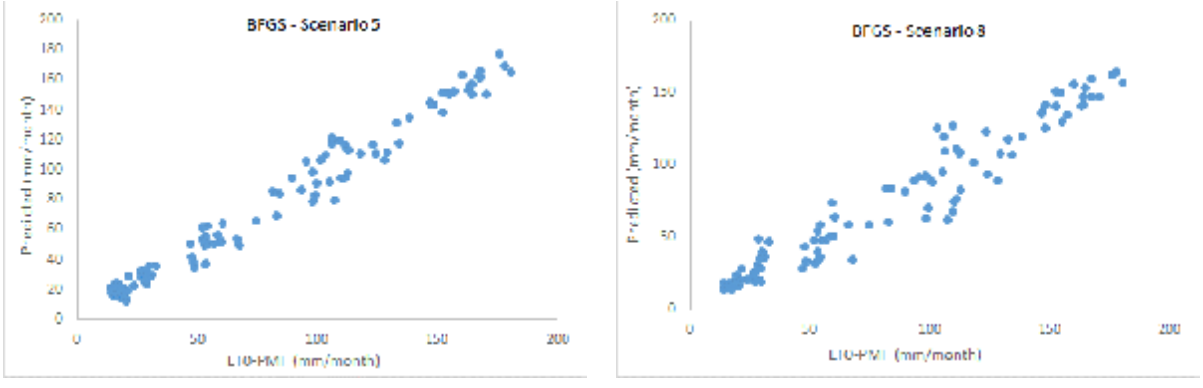

Figure 8. Scatter plots of Scenarios 5 and 8

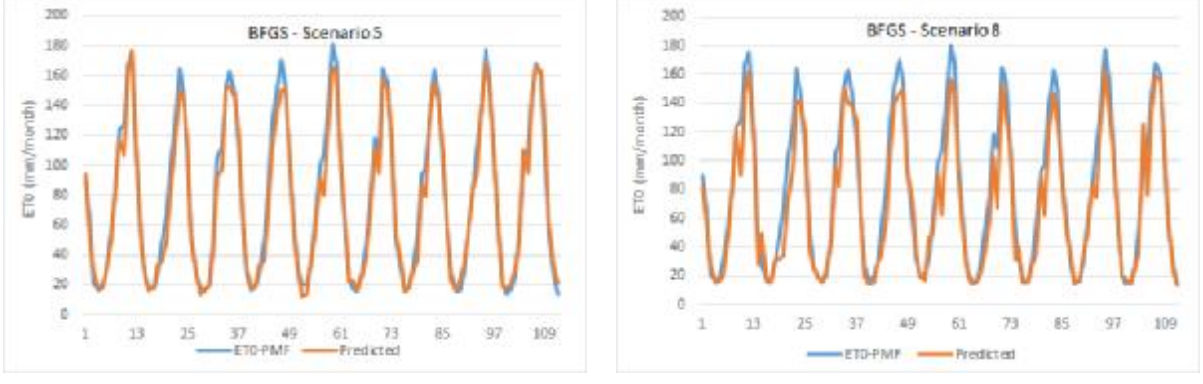

Figure 9. Time series graphics of Scenarios 5 and 8

https://doi.org/10.5194/hess-2020-224
Preprint. Discussion started: 22 July 2020


Hydrology and Earth System Sciences
Discussions

In this study, ET_0 amounts were estimated with the LSTM method, which is included in deep learning techniques. In the LSTM model used in this study, two hidden layers with 200 and 150 neurons, relu activation function, and Adam optimization were used. Learning rate alternatives from $1e^{-1}$ to $1e^{-9}$, Decay as $1e^{-1}$ to $1e^{-9}$, and 500-750-1000 as epoch have been tried. The best results obtained for 10 different scenarios at the modeling stage according to the LSTM method are given in Table 7.

Table 7. Results obtained with LSTM method

Scenario No	Evaluation metrics		
	R	MAE	RMSE
1	0.9884	8.6232	11.4663
2	0.9800	8.5703	11.7467
3	0.9667	14.8644	17.1128
4	0.9692	11.5043	13.7417
5	0.9879	6.2907	8.5897
6	0.9799	8.1580	10.6059
7	0.9678	10.1113	13.6070
8	0.9687	11.6711	14.4864
9	0.9308	15.2565	19.4120
10	0.9602	13.7034	16.1857

As in other methods, the 5th and 8th scenarios of the LSTM model gave the best and most appropriate results. According to the results, the 5th scenario including TMean, TMin, TMax and n meteorological variables gave the best result (R = 0.9879, MAE = 6.2907 mm/month RMSE = 8.5897 mm/month). However, scenario 8 only gave the most appropriate result (R = 0.9687, MAE = 11.6711 mm/month, RMSE = 14.4864 mm/month) with the sunshine duration (n) meteorological variable. Scatter plot and time series graphs are drawn for the LSTM model are given in Figures 10 and 11. As can be seen, the LSTM method predicted ET_0 amounts with a high success rate, and a high level of agreement was achieved between the estimates obtained from the model and FAO56PM- ET_0 values.

https://doi.org/10.5194/hess-2020-224
Preprint. Discussion started: 22 July 2020

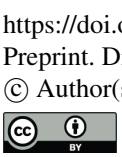

Hydrology and Earth System Sciences
Discussions
Open Access
EGU

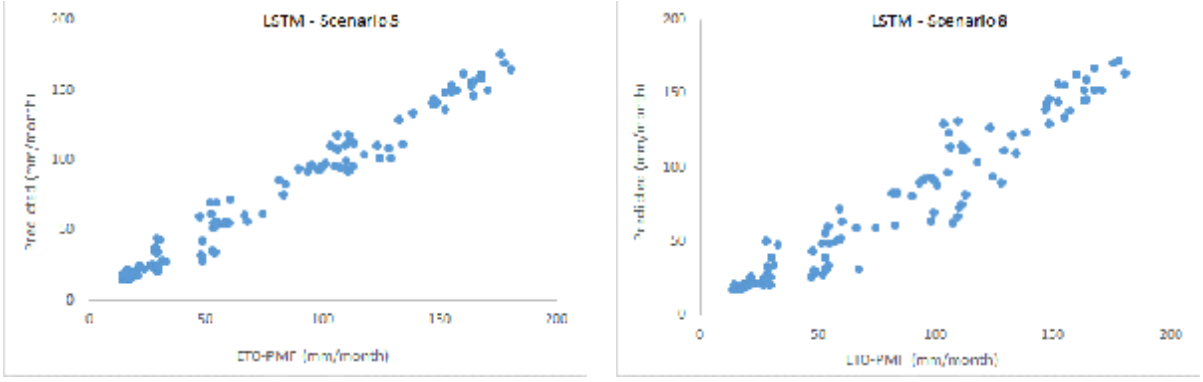

Figure 10. Scatter plots of scenarios 5 and 8

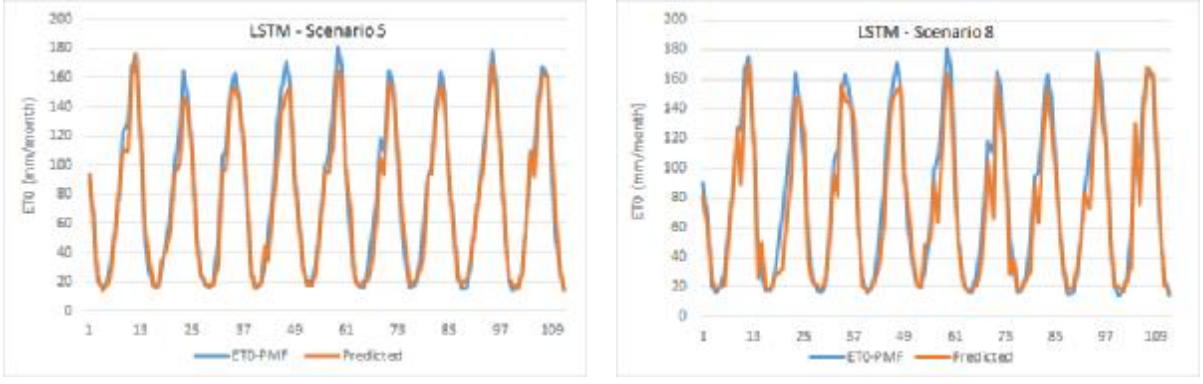

Figure 11. Time series graphics of Scenarios 5 and 8

In order to evaluate and compare the models used in this study, statistical values for the test phase are given in both FAO56PM-ET_0 and the models in Table 8.

Table 8. Statistical values of the test phase

	GPR		SVR		BFGS-ANN		LSTM		
Statistic	Scenario 5	Scenario 8	Scenario 5	Scenario 8	Scenario 5	Scenario 8	Scenario 5	Scenario 8	ET_0PM
Minimum	17.687	19.1090	15.1900	17.1520	12.2480	13.9060	14.2971	16.9787	13.99
Maximum	163.440	158.557	180.530	167.527	176.765	164.100	175.613	172.767	180.53
Mean	75.8818	71.3861	74.5771	71.2124	75.8644	70.7299	75.6023	72.3210	79.21
Stdev	48.8941	47.6359	51.5342	48.9192	50.6812	48.2539	50.0143	50.2075	53.26
Correlation	0.9820	0.9691	0.9885	0.9691	0.9890	0.9710	0.9879	0.9687	1
Number of records	112	112	112	112	112	112	112	112	112

https://doi.org/10.5194/hess-2020-224
Preprint. Discussion started: 22 July 2020

Hydrology and Earth System Sciences
Discussions

As can be seen from this table, the closest value to FAO56PM-ET_0 minimum value (13.99 mm/month) is 8th scenario in BFGS-ANN method (13.906 mm/month); FAO56PM-ET_0 maximum value (180.53 mm/month) has been reached in the 5th scenario (180.53 mm/month) in SVR method which is the closest and even the same value. The value closest to the mean value of FAO56PM-ET_0 (79.21 mm/month) belongs to the 5th scenario (75.8818 mm/month) in the GPR method; the value closest to the FAO56PM-ET_0 Stdev value (53.26 mm/month) is the value of the 5th scenario (51.5342 mm/month) in the SVR method. If the models are ranked according to the correlation coefficient, the best results were BFGS-ANN, SVR, LSTM, and GPR in the 5th scenario and BFGS-ANN, GPR, SVR, and LSTM in the 8th scenario. As can be seen from the table, all methods have estimated the ET_0 amounts to be acceptable, all with little difference.

To evaluate the models with the help of diagrams besides the tables, Taylor diagram for the 5th and 8th scenarios is given in Figure 12. As can be understood from the figure, all four methods used follow one another with a slight difference, but BFGS-ANN seems to achieve higher success than others. When looking at the histogram graph (Figure 1.), it is seen that FAO56PM-ET_0 values do not conform to normal distribution. This mismatch is considered to be the reason why the GPR method is relatively less successful than other methods.

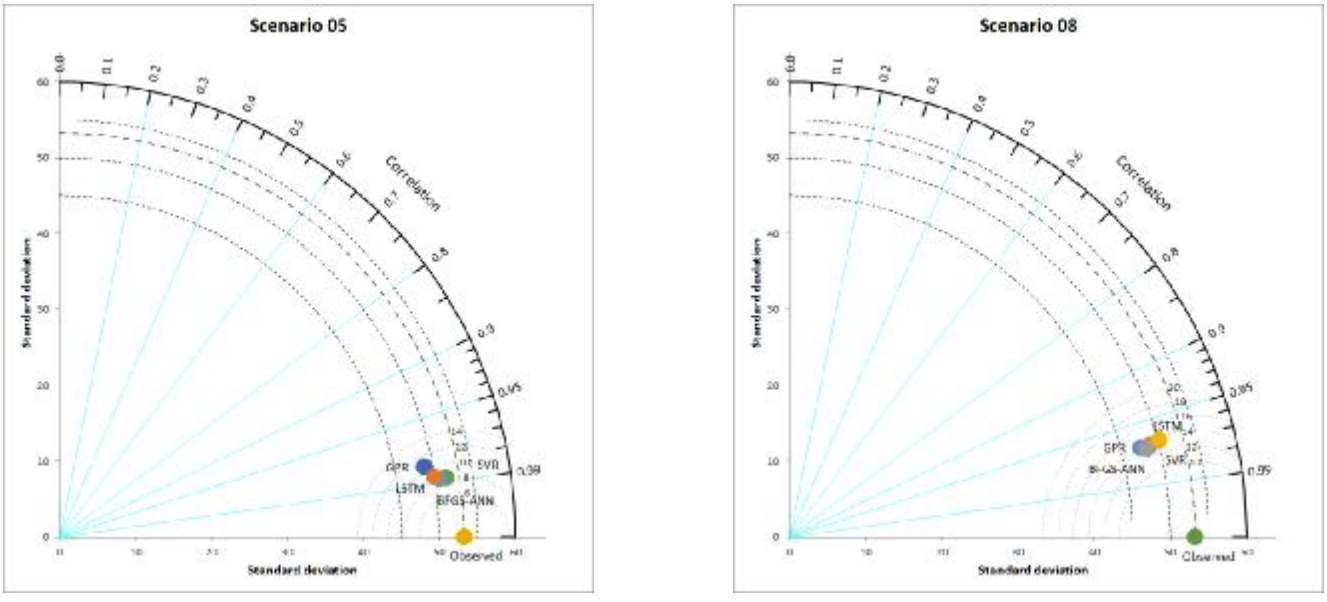

Figure 12. Taylor diagrams of Scenarios 5 and 8

https://doi.org/10.5194/hess-2020-224
Preprint. Discussion started: 22 July 2020


Hydrology and Earth System Sciences
Discussions

5. Conclusion

The amount of ET_0 can be calculated with many experimental equations. However, these equations can generally differ spatially and also contain many parameters. Since ET_0 contains a complex and nonlinear structure, it can be easily estimated with the previously measured data without requiring a lot of parameters with ML methods. In this study, the estimation of the amount of ET_0 with a different machines and deep learning methods was made by using the least meteorological variable in the Corum region, which arid and semi-arid climate with Turkey has an important place in terms of agriculture. In this context, firstly, ET_0 amounts were calculated with the Penman-Monteith method and taken into consideration as the output of the models used. Then, 10 different scenarios were created including the average, highest and lowest temperatures, sunshine duration, wind speed, average, highest, and lowest relative humidity meteorological variables. Kernel-based GPR and SVR methods, BFGS-ANN, and LSTM models are used and ET_0 amounts are estimated. According to the results obtained, the BFGS-ANN model performed better than others, although all four methods used predicted ET_0 amounts in acceptable accuracy and error levels. In kernel-based methods (GPR and SVR), PUK was the most successful kernel function. Besides, the 5th scenario, which is related to temperature and includes four meteorological variables such as average, highest and lowest temperature, and sunshine duration, gave the best results in all the scenarios used. After the 5th scenario, the 8th scenario, which includes only the duration of the sun, was determined as the most suitable scenario. In this case, the ET_0 amount was estimated using only sunshine duration without the need for other meteorological parameters for the study area. The Corum region is described as arid and semi-arid as the rainfalls are low. In a sense, this means that the cloudiness is low and the sunshine duration is long. The reason for the models to give quite good results by using only n value is a long time in the work area. Continuous measurement of meteorological variables in large farmland is a costly process that requires expert personnel, time, or good equipment. At the same time, some equations used for ET_0 calculations are not preferred by specialists because they contain many parameters. In this case, it is very advantageous for water resources managers to estimate ET_0 amounts only with the help of sunbathing time, which is easy to measure and requires no extra cost.

Funding Acknowledgement

This work was supported by Fellowships for Visiting Scientists and Scientists on Sabbatical Leave Programme (2221) of The Scientific and Technological Research Council of Turkey (TUBITAK).

Author Contributions: Conceptualization, M.T.S., and H.A.; Data curation, M.T.S., H.A.; Formal analysis, S.S.; Funding acquisition, H.A., M.T.S.; Investigation, M.T.S., H.A. and S.S.; Methodology, M.T.S., H.A. and S.S.; Project administration, H.A.; Resources, M.T.S. and H.A.; Software, M.T.S. A.M. and H.A.; Supervision, M.T.S, H.A..; Validation, A.M.. and S.S.; Visualization, M.T.S., H.A. and S.S.; Writing—original draft, M.T.S., H.A. and S.S.; Writing—review and editing, M.T.S. A.M. and S.S. All authors have read and agreed to the published version of the manuscript.

Conflicts Of Interest: The authors declare no conflict of interest.

Code/Data availability: Data are available on request due to privacy or other restrictions

https://doi.org/10.5194/hess-2020-224
Preprint. Discussion started: 22 July 2020


Hydrology and Earth System Sciences
Discussions

References

Abrishami, N., Sepaskhah, A.R., Shahrokhnia, M.H. 2019. Estimating wheat and maize daily evapotranspiration using artificial neural network. Theor. Appl. Climatol. 135, 945–958. https://doi.org/10.1007/s00704-018-2418-4

Anonymous. 2017. Agricultural data of Corum province (In Turkish). Corum province Food Agriculture Livestock Directorate

Arnulf B. A. Graf, S. Borer. 2001. Normalization in Support Vector Machines, Lecture Notes in Computer Science, 2191: 277-282.

Banda, P., Cemek, B., Kucukktopcu, E. 2018. Estimation of daily reference evapotranspiration by neuro computing techniques using limited data in a semi-arid environment. Arch. Agron. Soil Sci. 64, 916–929. https://doi.org/10.1080/03650340.2017.1414196

Brownlee, J. 2020. How to Develop LSTM Models for Time Series Forecasting. Retrieved from https://machinelearningmastery.com/how-to-develop-lstm-models-for-time-series-forecasting/

Citakoglu, H., Cobaner, M., Haktanir, T., Kisi, O. 2014. Estimation of Monthly Mean Reference Evapotranspiration in Turkey. Water Resour. Manag. 28, 99–113. https://doi.org/10.1007/s11269-013-0474-1

Curtis, F.E., Que, X., 2015. A quasi-Newton algorithm for nonconvex, nonsmooth optimization with global convergence guarantees. Math. Program. Comput. 7, 399–428. https://doi.org/10.1007/s12532-015-0086-2

Doorenbos, J. and Pruitt, W.O. 1977. Crop Water Requirements. FAO Irrigation and Drainage Paper 24, FAO, Rome, 144 p.

Fan, J., Yue, W., Wu, L., Zhang, F., Cai, H., Wang, X., Lu, X., Xiang, Y., 2018. Evaluation of SVM, ELM and four tree-based ensemble models for predicting daily reference evapotranspiration using limited meteorological data in different climates of China. Agric. For. Meteorol. 263, 225–241. https://doi.org/10.1016/j.agrformet.2018.08.019

Feng, Y., Cui, N., Zhao, L., Hu, X., Gong, D., 2016. Comparison of ELM, GANN, WNN and empirical models for estimating reference evapotranspiration in humid region of Southwest China. J. Hydrol. 536, 376–383. https://doi.org/10.1016/j.jhydrol.2016.02.053

Feng, Y., Peng, Y., Cui, N., Gong, D., Zhang, K., 2017. Modeling reference evapotranspiration using extreme learning machine and generalized regression neural network only with temperature data. Comput. Electron. Agric. 136, 71–78. https://doi.org/10.1016/j.compag.2017.01.027

Fletcher R. 1987. Practical methods of optimization (2nd ed.), New York: John Wiley & Sons, ISBN 978-0-471-91547-8, Wiley.

Rasmussen, CE. and Williams, CKI. 2005. Gaussian Processes for Machine Learning (Adaptive Computation and Machine Learning series).

Gavili, S., Sanikhani, H., Kisi, O., Mahmoudi, M.H., 2018. Evaluation of several soft computing methods in monthly evapotranspiration modelling. Meteorol. Appl. 25, 128–138. https://doi.org/10.1002/met.1676

Gocić, M., Motamedi, S., Shamshirband, S., Petković, D., Ch, S., Hashim, R., Arif, M., 2015. Soft computing approaches for forecasting reference evapotranspiration. Comput. Electron. Agric. 113, 164–173. https://doi.org/10.1016/j.compag.2015.02.010

Hsu, C.W., Chang, C.C., Lin, C.J., 2010, A Practical Guide to Support Vector classification, http://www.csie.ntu.edu.tw/~cjlin/papers/guide/guide.pdf.

Kavzoglu, T. and Colkesen, I. 2010. Investigation of the Effects of Kernel Functions in Satellite Image Classification Using Support Vector Machines. Harita Dergisi Temmuz 2010 Sayi 144

Le, X.-H., Ho, H. V., Giha, L., & Sungho, J. 2019. Application of Long Short-Term Memory (LSTM) Neural Network for Flood Forecasting. Water. https://doi.org/10.3390/w11071387

Nema, M.K., Khare, D., Chandniha, S.K., 2017. Application of artificial intelligence to estimate the reference evapotranspiration in sub-humid Doon valley. Appl. Water Sci. 7, 3903–3910. https://doi.org/10.1007/s13201-017-0543-3

Nocedal, J. & Wright, S. 2006, Numerical Optimization. 664 p. Springer. DOI: 10.1007/978-0-387-40065-5

Pandey, P.K., Nyori, T., Pandey, V., 2017. Estimation of reference evapotranspiration using data driven techniques under limited data conditions. Model. Earth Syst. Environ. 3, 1449–1461. https://doi.org/10.1007/s40808-017-0367-z

Reis, M.M., da Silva, A.J., Zullo Junior, J., Tuffi Santos, L.D., Azevedo, A.M., Lopes, É.M.G., 2019. Empirical and learning machine approaches to estimating reference evapotranspiration based on temperature data. Comput. Electron. Agric. 165, 104937. https://doi.org/10.1016/j.compag.2019.104937

Saggi, M.K., Jain, S., 2019. Reference evapotranspiration estimation and modeling of the Punjab Northern India using deep learning. Comput. Electron. Agric. 156, 387–398. https://doi.org/10.1016/j.compag.2018.11.031

Sattari, M.T., Pal, M., Yurekli, K., Unlukara, A., 2013. M5 model trees and neural network based modelling of ET0 in Ankara, Turkey. Turkish J. Eng. Environ. Sci. 37, 211–220. https://doi.org/10.3906/muh-1212-5

Shabani, S., Samadianfard, S., Sattari, M.T., Mosavi, A., Shamshirband, S., Kmet, T., Várkonyi-Kóczy, A.R., 2020. Modeling Pan Evaporation Using Gaussian Process Regression K-Nearest Neighbors Random Forest and Support Vector Machines; Comparative Analysis. Atmosphere (Basel). 11, 66. https://doi.org/10.3390/atmos11010066

Shamshirband, S., Amirmojahedi, M., Gocić, M., Akib, S., Petković, D., Piri, J., Trajkovic, S., 2016. Estimation of Reference Evapotranspiration Using Neural Networks and Cuckoo Search Algorithm. J. Irrig. Drain. Eng. 142, 04015044. https://doi.org/10.1061/(ASCE)IR.1943-4774.0000949

Taylor, K.E., 2001. Summarizing multiple aspects of model performance in a single diagram. J. Geophys. Res. Atmos. 106, 7183–7192. https://doi.org/10.1029/2000JD900719

Vapnik, V. 2013. The Nature of Statistical Learning Theory; Springer Science & Business Media: Berlin, Germany.

Wang, P., Liu, C., Li, Y., 2019. Estimation method for ET0 with PSO-LSSVM based on the HHT in cold and arid data-sparse area. Cluster Comput. 22, 8207–8216. https://doi.org/10.1007/s10586-018-1726-x

https://doi.org/10.5194/hess-2020-224
Preprint. Discussion started: 22 July 2020


Hydrology and Earth System Sciences
Discussions

Wen, X., Si, J., He, Z., Wu, J., Shao, H., Yu, H., 2015. Support-Vector-Machine-Based Models for Modeling Daily Reference Evapotranspiration with Limited Climatic Data in Extreme Arid Regions. Water Resour. Manag. 29, 3195–3209. https://doi.org/10.1007/s11269-015-0990-2

Wu, L., Peng, Y., Fan, J., Wang, Y., 2019. Machine learning models for the estimation of monthly mean daily reference evapotranspiration based on cross-station and synthetic data. Hydrol. Res. 50, 1730–1750. https://doi.org/10.2166/nh.2019.060

Zhang, Y., Wei, Z., Zhang, L., Du, J., 2019. Applicability evaluation of different algorithms for daily reference evapotranspiration model in KBE system. Int. J. Comput. Sci. Eng. 18, 361. https://doi.org/10.1504/IJCSE.2019.099074